European Journal of Pharmaceutical Sciences 184 (2023) 106402

Contents lists available at ScienceDirect

European Journal of Pharmaceutical Sciences

journal homepage: www.elsevier.com/locate/ejps

Development of a population pharmacokinetic model and optimal dosing regimen of leflunomide in Korean population

Yesong Shin [a,b], Dongwoo Chae [a], Kyungsoo Park [a,*]

[a] Department of Pharmacology, Yonsei University College of Medicine, Seoul 03722, Korea
[b] Brain Korea 21 Plus Project for Medical Science, Yonsei University, Seoul 03722, Korea

ARTICLE INFO

Keywords:
Leflunomide
Population pharmacokinetic model
Allometry
Enterohepatic circulation
Dose optimization

ABSTRACT

Purpose: Leflunomide is an immunosuppressive drug indicated for the treatment of rheumatoid arthritis (RA). While the pharmacokinetics (PK) of its active metabolite A771726 reportedly show large interindividual variability, no efficient dose individualization strategy is currently available. The goal of this work was to develop a population PK model for A771726 and propose an optimal individualized dosing strategy.
Methods: A771726 plasma concentration data were collected from 50 healthy male volunteers participating in two leflunomide PK studies given a single oral dose of 40 mg. Concentrations were elevated in low body weight (WT) subjects and showed multiple peaks. Thus, A771726 PK modeling was conducted incorporating allometry scaling and enterohepatic circulation (EHC). For dose optimization, simulating a set of 1000 virtual subjects from the developed model and dividing the subjects into 5 groups with WT of 50, 60, 70, 80, 90 kg, respectively, the optimal dose was explored that achieves the drug concentration most similar to the target, which was defined as the concentration for the 70 kg subject treated with the current standard dosage regimen (the loading dose of 100 mg QD for 3 days, followed by the maintenance dose of 20 mg QD).
Results: The data were best described by a two compartment model with first order absorption incorporating EHC with the bile released into the intestine. None of the covariates tested was found to be significant other than WT used in allometry. Simulation showed that the optimal loading dose increased by 15 mg for every 10 kg increment in WT while the optimal maintenance dose was 15 and 25 mg for 50 and 90 kg groups, respectively, and the same (= 20 mg) for the others. Large concentration differences from the target observed in low and high WT groups disappeared when optimal doses were given.
Conclusions: This work demonstrates the importance of a population PK model-based dose optimization approach in maintaining drug therapeutic concentrations in leflunomide treatment.

1. Introduction

Leflunomide [N-(4-trifluoromethylphenyl)−5-methylisoxazol-4-carboxamide] is an isoxazole derivative and an immunomodulatory agent, which inhibits dihydroorotate dehydrogenase (DHODH) and T-cell pyrimidine biosynthesis, thereby suppressing T-cell proliferation. Leflunomide was approved by the U.S. FDA in September 1998 as a dose-modifying anti-rheumatic drug (DMARD) to improve and delay the symptoms and progression of rheumatoid arthritis (RA) treated with or without methotrexate (Weinblatt et al., 1999).

Leflunomide is a pro-drug that does not have therapeutic activity. Following oral administration, leflunomide is nearly completely absorbed in man (Sandoz Canada, 2016) and almost completely converted into a major active metabolite A771726 [2-cyano-3-hydroxy-N-(4-trifluoromethylphenyl)-crotonamide], also known as teriflunomide or M1 (Rozman, 2002). As a result, leflunomide itself is hardly detectable in plasma (Rozman, 2002; Sanofi-Aventis, 1998). A771726 inhibits the proliferation of activated T-lymphocytes by acting specifically on DHODH to reduce pyridine (uridine monophosphate (rUMP) biosynthesis (2012; Rozman, 2002; Sanofi-Aventis, 1998).

Leflunomide is characterized by high protein binding and its metabolite is known to show multiple peaks in the concentration-time profile due to enterohepatic circulation (EHC), which may contribute to its long half-life (~2 weeks) (2012; Rozman, 2002; Sanofi-Aventis, 1998). For this reason, FDA recommended a loading dose of 100 mg QD for 3 days to reach rapid steady-state concentration levels

* Corresponding author.
E-mail address: kspark@yuhs.ac (K. Park).

https://doi.org/10.1016/j.ejps.2023.106402
Received 15 August 2022; Received in revised form 1 February 2023; Accepted 5 February 2023
Available online 6 February 2023

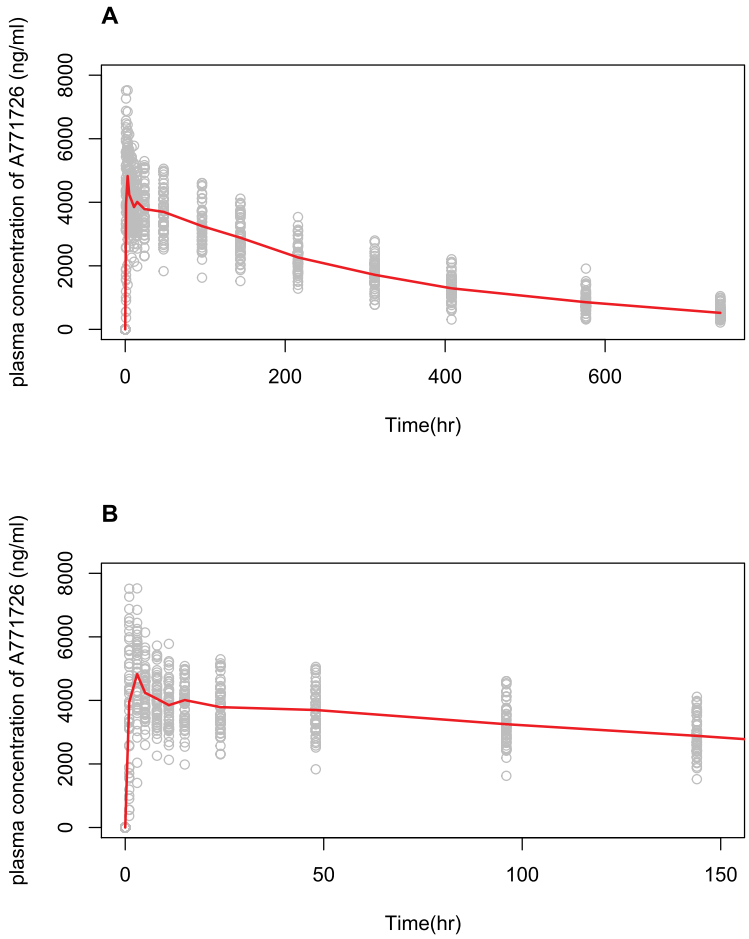

Fig. 1. Plasma concentrations versus time for A771726, the active metabolite of leflunomide, for (A) the entire time period and (B) the early period for $t \leq 144$ hour where Figure (B) was presented to focus on the time interval where multiple peaks occurred. In the figure, dots represent observations and the solid line represents a regression line.

(Sanofi-Aventis, 1998).

However, therapeutic failure to leflunomide has been observed in a significant proportion of patients; it has been reported that approximately 52% of RA patients show an inadequate response to leflunomide (Fajardo-Robledo et al., 2022) and more than half of patients discontinue leflunomide treatment within a year, mainly due to adverse drug reactions (van Roon et al., 2005).

While various factors could be related to the failure of leflunomide treatment in RA, it has been reported that if A771726 concentration is less than 16 mg/L there is no therapeutic effect, suggesting what is the most significantly related is suboptimal drug concentration (Mladenovic et al., al.,1995; van Roon et al., 2005). This implies the importance of a pharmacokinetic (PK) model for dose individualization to avoid leflunomide treatment failure. Several PK models of leflunomide have been published to date (Bohanec Grabar et al., 2009; Chan et al., 2005; Shi et al., 2005; W. Weber, 1997), which, however, are limited in that EHC contributing to the long half-life of the metabolite was not taken into account. A model incorporating EHC or physiologically based PK model has been reported (Hopkins et al., 2015; Yao et al., 2019), and an optimal population dose has been used in a phase II trial (Hopkins et al., 2015). However, no attempt has been made to propose an individualized dosing regimen.

The aim of this study was thus to develop a population PK model of A771726, identify significant patient covariates, and propose an optimal individualized dosing regimen.

2. Methods

2.1. Subjects and data

The data were obtained from two clinical studies investigating leflunomide PK in Korean population, which were conducted at Yonsei University Severance Hospital under the approval of the Institutional Review Board of Severance Hospital (Approval No: 4–2007–0172, 4–2007–0276).

In those studies, subjects were recruited who were considered healthy based on the medical history, physical examination, and laboratory tests. Selection criteria were age between 19 and 40 years and no chronic diseases. Exclusion criteria included a previously administrated drug metabolism enzyme inducer or inhibitor, which may influence the PK of the study drug, and an immunosuppressant which may interact with the study drug. Subjects who had history of serious infection, organ, bone marrow transplant, tuberculosis, or liver disease and those who had alanine aminotransferase >50 IV/L, serum creatinine >1.5 mg/dL, or high blood pressure were also excluded.

Each subject then received a single oral dose of 40 mg of leflunomide (Arava® 20 mg 2 tablets) (Sanofi, Paris, France) under fasting condition at 8 am on Day 1. Blood samples for PK analysis were collected at predose, 1, 3, 5, 8, 11, 15, 24, 48, 96, 144, 216, 313, 408, 576, and 744 h after administration.

2.2. Bioanalysis

Since concentration of leflunomide could not be measured due to immediate metabolism, the concentration of A771726, the active metabolite of leflunomide, was analyzed using a Liquid Chromatography-Tandem Mass Spectrometery (LC/MS/MS) system, composed of HPLC (Shimadzu) and a Triple quadrupole mass spectrometer (Applied Biosystem). The spectrometer used the multiple reaction monitoring (MRM) mode of negative electro spray ionization (ESI), which transmitted at (m/z) 269.0 → 160.0 for standard material, A771726, and 273.1 → 164.3 for internal standard material, A771726-d4. The column used were Capcell pak C18 UG120V (5 μm, 150 × 2.0 mm i.d., Shiseido). The concentrations were quantified in 10 mM ammonium acetate (adjusted to pH = 4.5 with acetic acid)/acetonitrile (22:78, v/v) for mobile phase, with a flow rate of 0.5 ml/min. The peak area ratio of A771726 to the internal standard material was calculated, and the concentration of A771726 in the plasma was calculated from the pre-written calibration line which shows linearity(r = 0.9990) in the range 200 ~ 20,000 ng/ml.

2.3. Model development

2.3.1. Structural model

A771726 plasma concentrations were modeled by testing one- and two-compartment disposition models, with zero-order, first-order and parallel zero- and first-order absorptions, and first-order elimination.

For disposition models, clearance (CL) and volume of distribution (V) were parameterized using allometric scaling as (Holford et al., 2013; West et al., 1997)

$$CL = CL_{STD} \cdot (WT/WT_{STD})^{0.75}$$

$$V = V_{STD} \cdot (WT\ /\ WT_{STD})$$

where CL_{STD} and V_{STD} denote CL and V for subjects with WT = WT_{STD}, respectively, with WT being the body weight and WT_{STD} being the standard body weight (= 70 kg).

When inspecting individual concentration profiles, we noticed multiple peaks as seen in Fig. 1 (first peak at 3 h and second peak at 15 h), suggestive of EHC. Thus, based on previous studies (Hopkins et al., 2015), we incorporated EHC into the model using the gallbladder compartment, assuming the emptying process of the gallbladder into the intestine, rather than directly into the blood (Ibarra et al., 2021; Roberts et al., 2002; Soulele and Karalis, 2019). In doing so, we assumed that gallbladder emptying occurred during the following time intervals:

$$4 \le \mathrm{MODT} < 4 + \mathrm{T41},\ 10 \le \mathrm{MODT} < 10 + \mathrm{T41},\ 23 \le \mathrm{MODT} < 23 + \mathrm{T41}$$

where 4, 10, and 23 refer to post-dose times, corresponding to clock times of 12 pm, 6 pm, and 7 am next day, respectively, meal times were 12 pm for lunch, 6 pm for dinner, and 7 am for breakfast, MODT refers to time modulo 24, and T41 refers to the duration of gallbladder emptying, which was estimated.

2.3.2. Statistical model

Random effects associated with inter-individual differences in PK parameters were assumed to follow a log-normal distribution. PK parameters were thus formulated as follows:

$$P_i = P_{TV} \cdot e^{\eta_i}$$

P is an arbitrary parameter, P_i and P_{TV} are individual and typical parameter values, respectively, and η_i is the inter-individual random effect following a normal distribution with mean zero and variance ω_i^2. The residual variability was incorporated as follows:

$$Y_{ij} = F_{ij} \cdot (1 + \varepsilon_{pro,ij}) + \varepsilon_{add,ij}$$

Y_{ij} and F_{ij} are observed and predicted concentration for individual i at the time point j, respectively, and $\varepsilon_{pro,ij}$ and $\varepsilon_{add,ij}$ are proportional and additive residual errors flowing a normal distribution with mean zero and variance σ_{pro}^2 and σ_{add}^2, respectively.

2.4. Covariate analysis

Stepwise covariate model building based on a likelihood ratio test was conducted for covariate search. The selection criteria for forward addition was $p < 0.05$, and backward deletion $p < 0.01$. The tested covariates were age, smoking status (yes/no), alcohol consumption (yes/no), and caffeine intake (yes/no). We evaluated the relationship between covariates and parameters with linear and exponential models.

2.5. Model evaluation

We considered goodness of fit plots and physiological plausibility as well as the objective function value (OFV) in selecting the final model. The reliability of the final model was further assessed by comparing parameter estimates and their standard errors with bootstrap analysis results obtained from 1000 replicates of data. The final model was then evaluated using visual predictive check (VPC) whereby 1000 datasets were generated from the final model and compared with the observed concentrations to assess their concordance.

2.6. Simulation

With the final model selected, simulation was performed to develop the optimal dosing regimen for leflunomide to propose as a practical strategy for dose individualization. We defined the optimal dosing regimen as that maximizing the chances of attaining the target concentration in each covariate group. The target concentration was defined as the steady state A771726 concentration predicted from the final model developed, given the current standard regimen of loading dose of 100 mg QD for 3 days followed by maintenance dose of 20 mg QD in a typical 70 kg subject (Chan et al., 2005).

Generating 1000 virtual subjcacts from the developed model in each covariate group, an optimal loading dose was obtained by minimizing the expected error below.

$$Err_L\ (\%) = \frac{E\{abs(C_{Test,L} - C_{Target,L})\}}{C_{Target,L}} \times\ 100$$

Where $C_{Target,L}$ is the target drug concentration for the loading dose, which was defined as the average of peak and trough concentrations in the 3rd dosing day (D3) predicted in a typical 70 kg patient who received the current standard regimen, $C_{Test,L}$ is the average drug concentration on D3 predicted for a test loading dose for a given covariate group, and $E\{\bullet\}$ denotes the expectation over the 1000 virtual subjects.

Then, an optimal maintenance dose was obtained by minimizing the expected error below.

$$Err_M\ (\%) = \frac{E\{abs(C_{Test,M} - C_{Target,M})\}}{C_{Target,M}} \times\ 100$$

Where $C_{Target,M}$ is the target drug concentration for the maintenance dose, which was defined as the average of peak and trough concentrations in the 56th dosing day (D56), based on that the steady state would be reached by D56 (4 half-lives) given the drug half-life of 14 days, predicted in a typical 70 kg patient who received the current standard regimen, and $C_{Test,M}$ is the average drug concentration on D56 predicted for a test maintenance dose for a given covariate group.

The search was performed with a step size of 5 mg for a range of loading doses from 65 to 140 mg and maintenance doses from 5 to 35

Table 1
Characteristics of study subjects ($N = 50$).

Continuous Variable	Mean ± SD	Median (Max – Min)
Age (years)	25.2 ± 3.83	25 (37 – 19)
Weight (kg)	71.2 ± 8.67	71 (91.5 – 54.3)
Binary Variable	**Yes**	**No**
Smoking	14 (28%)	36 (72%)
Alcohol	6 (88%)	44 (12%)
Caffeine	4 (92%)	46 (8%)

mg.

2.7. Software

Model building and evaluation were done with NONMEM 7.4 (ICON Development Solutions, Ellicott City, MD, USA) using the first-order conditional estimation with interaction (FOCE-I) method. VPCs were performed using Perl-speaks-NONMEM (PsN ver. 4.9.0) and Xpose 4 (ver. 4.0) in R (ver. 3.5.2; R Foundation for Statistical Computing, Vienna, Austria).

3. Results

3.1. Subject characteristics

Twenty-five male subjects were enrolled in each study, 50 in total. The demographics of the subjects are described in Table 1, with the mean age of 25 years and the mean body weight of 71 kg. There was no significant difference in subject demographic characteristics between the 2 study groups (data not shown).

3.2. Model development

With a gallbladder compartment incorporated, a two-compartment disposition model with first-order absorption was chosen based on the reasonable fit to the data as assessed by OFV and other model evaluation criteria described in Methods.

A schematic diagram of the model is shown in Fig. 2, which is formulated as shown below:

Outside the gallbladder emptying period:

$$\frac{dA1}{dt} = -ka \times A1$$

$$\frac{dA2}{dt} = ka \times A1 - \frac{CL}{V2} \times A2 - k24 \times A2 + \frac{Q}{V3} \times A3 - \frac{CL}{V2} \times A2$$

$$\frac{dA3}{dt} = \frac{CL}{V2} \times A2 - \frac{Q}{V3} \times A3$$

$$\frac{dA4}{dt} = k24 \times A2$$

During the gallbladder emptying period:

$$\frac{dA1}{dt} = -ka \times A1 + \frac{A4}{T41}$$

$$\frac{dA2}{dt} = ka \times A1 - \frac{CL}{V2} \times A2 - k24 \times A2 + \frac{Q}{V3} \times A3 - \frac{CL}{V2} \times A2$$

$$\frac{dA3}{dt} = \frac{CL}{V2} \times A2 - \frac{Q}{V3} \times A3$$

$$\frac{dA4}{dt} = k24 \times A2 - \frac{A4}{T41}$$

where variable names are defined as follows:

A1, gastric intestinal (GI) tract; A2, central compartment; A3, peripheral compartment; A4, gallbladder compartment; V2, volume of central compartment; V3, volume of peripheral compartment; ka, absorption rate constant from GI tract to central compartment; CL, systemic clearance; Q, inter-compartment clearance (k23 = Q/V2, k32 = Q/V3); k24, transfer rate constant from central to gallbladder compartment; T41, duration of gallbladder emptying (k41 = 1/T41).

Table 2
Parameter estimates of the final PK model of A77 1726.

Parameter	Estimates (RSE%)	Bootstrap Median (RSE%)	Bootstrap 95% CI
Structural Parameters			
ka (h^{-1})	1.61 (15.22)	1.524 (31.67)	1.16 - 2.184
CL (L/h)	0.0273 (3.883)	0.0274 (0.111)	0.026 - 0.029
Q (L/h)	0.593 (19.73)	0.594 (19.06)	0.236 - 0.926
V2 (L)	6.83 (5.534)	6.734 (34.38)	6.144 - 7.231
V3 (h)	2.27 (4.978)	2.254 (56.95)	0.804 - 2.951
k24 (h^{-1})	0.0116 (20.6)	0.0132 (1.364)	0.006 - 0.054
T41 (h)	4 (0.034)	4.00 (48.08)	4 - 5.001
Inter-individual Variability			
ω^2_{ka} (h^{-1})	107.2% (11.22)	101.7% (7.00)	79.4% - 130.28%
ω^2_{CL} (L/h)	27.22% (10.26)	27.33% (11.18)	21.72% - 32.42%
ω^2_{Q} (h^{-1})	0 FIX	0 FIX	0 FIX
ω^2_{V2} (L)	24.7% (17.46)	24.17% (13.55)	19.02% - 30.35%
ω^2_{V3} (h)	0 FIX	0 FIX	0 FIX
ω^2_{k24} (h)	0 FIX	0 FIX	0 FIX
Residual Variability			
σ^2_{PRO} (CV%)	10.91% (12.61)	10.78% (18.68)	8.53% - 12.79%
σ^2_{ADD} (SD)	50.89 (69.88)	56.67 (1.98)	18.9 - 117.49

ka, absorption rate constant from depot to central compartment; CL, systemic clearance; Q, inter-compartmental clearance; V2, central volume of distribution; V3 peripheral volume of distribution; k24, transfer rate constant from central to gallbladder compartment; T41, duration of gallbladder emptying; ω^2, variance of inter-individual random effect; σ^2_{PRO}, variance of proportional residual error; σ^2_{ADD}, variance of additive residual error.

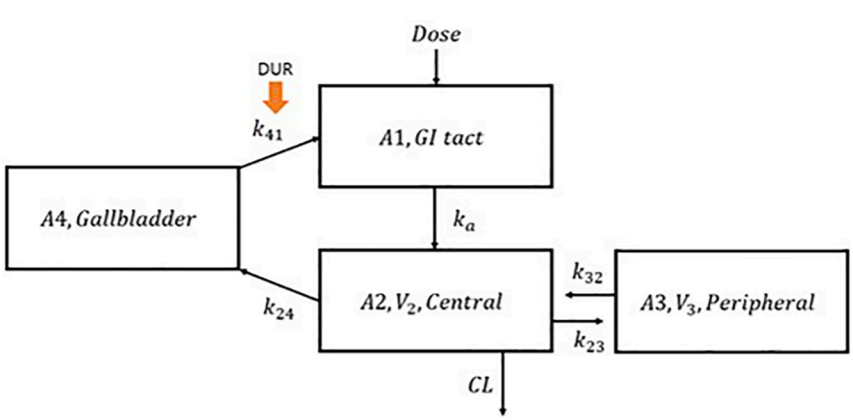

Fig. 2. A schematic diagram of the pharmacokinetic model of A771726. In the diagram, A1, A2, A3 and A4 represent the amount of A771726 in the gastric intestinal (GI) tract, central compartment, peripheral compartment, and gallbladder compartment, respectively, V2 and V3 represent the volume of distribution for central and peripheral compartment, respectively, ka represents the absorption rate constant from GI tract to central compartment, CL and Q represent the systemic and inter-compartment clearance (k23 = Q/V2, k32 = Q/V3), respectively, k24 represents the transfer rate constant from central to gallbladder compartment, and T41 represents the duration of gallbladder emptying (k41 = 1/T41).

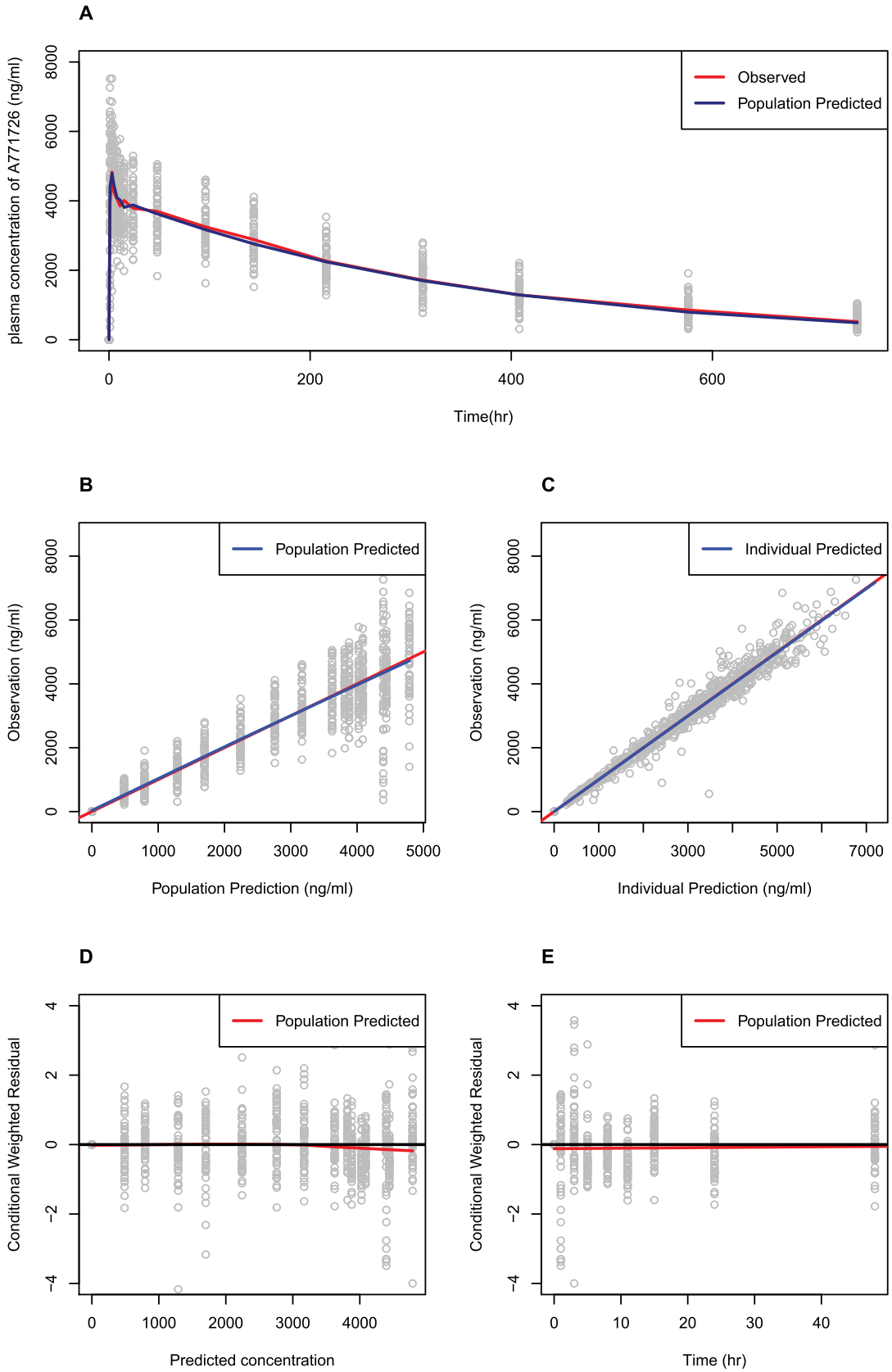

Fig. 3. Goodness-of-fit plots for the final population pharmacokinetic model of A771726. (A) Plasma concentrations versus time where dots represent observations, the red line represents a smoother line of observations, and the blue line represents the population prediction; (B, C) Observations vs population and individual predictions where dots represent concentrations, the blue line represents a smoother line, and the red line represents the line of identity; (D, E) Conditional weighted residuals vs population predictions and time where dots represent residuals, the red line represents a smoother line, and the black line represents the line of identity.

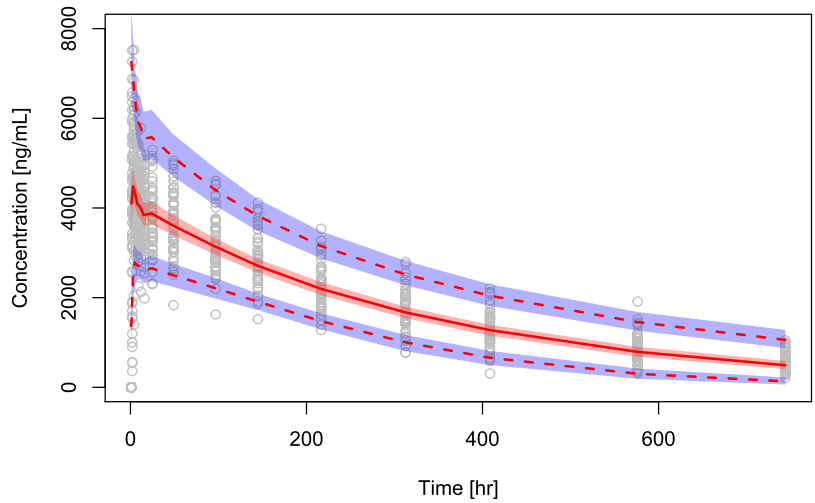

Fig. 4. Visual predictive checks of the final PK model for A771726. Dots represent observations, solid and dashed lines represent the median and 5% / 95% model predicted values, respectively. The red shaded area represents the 95% confidence interval on the model predicted median, and blue shaded areas represent the 95% confidence intervals on the predicted 5% and 95% values.

3.3. Covariate analysis

None of the covariates tested was found to influence model parameters significantly. While age influenced CL and smoking K12, they slightly failed to reach statistical significance ($p = 0.068$ and 0.078, respectively).

Thus, the final model only included WT via allometry, and the parameter estimates were for absorption, 1.61 h^{-1} for ka; for clearance, 0.0273 L/h for CL and 0.593 L/h for Q; for volume of distribution, 6.83 L for V2 and 2.27 L for V3; for EHC parameters, 0.0116 h^{-1} for k24 and 4 h for T41. This yielded the elimination rate constant of 0.004 h^{-1} (= CL/V2 = 0.0273/6.83), thereby producing the elimination half-life of 173 h (= 0.693/0.004), and the transfer half-life of 60 h (= 0.693/0.0116).

The inter-individual variability estimates were 24.7% for V2, 27.22% for CL, and 107.2% for ka. For the precision of parameter estimates, relative standard errors were all within 30% The estimated parameters of the final model are shown in Table 2.

3.4. Model evaluation

In Fig. 3, goodness-of-fit plots are presented, where it is seen that A771726 population and individual predictions well represented the observed data (Fig. 3:B, C). Conditional weighted residual errors showed no specific trends with regards to predicted concentration and time (Fig. 3:D, E). Some deviations at 1, 3 and 5 h (Fig. 3:E) might be due to high intra-individual variability or assay error that can be seen in oral drugs in the initial distribution phase and at near Tmax, which in our case was 3.5 h (data not shown). When evaluated by individual predictions versus time, the final model also represented the observed data well (Supplementary Fig. S1), and for inter-individual random effects, their histograms were close to the shape of normal distribution as expected and normal quantile-quantile (QQ) values well matched with theoretical ones (Supplementary Fig. S2), further confirming the appropriateness of the model. Parameter medians and 95% CIs obtained from bootstrap analyses are shown in Table 2. (Gastonguay et al., 2005). Parameter estimates obtained from the final model were close to bootstrap median values and all were included in bootstrap 95% CI, indicating the reliability of the final model parameters.

The VPC plot of the final model is reported in Fig. 4, showing that most of the observed concentrations fell within the 95% CI of the corresponding model predicted percentiles.

Table 3
The exploration of optimal loading and maintenance doses given QD in each weight (WT) group where Err denotes the error between target and achieved concentrations (see Methods for detail) and the asterisk (*) represents selected optimal dose.

Loading Dose							
WT = 50 kg (n = 1000)		WT = 60 kg (n = 1000)		WT = 80 kg (n = 1000)		WT = 90 kg (n = 1000)	
Dose (mg)	Err (%)	Dose (mg)	Err (%)	Dose (mg)	Err (%)	Dose (mg)	Err (%)
65	10.7	80	7.05	110	3.42	120	6.07
70 *	2.89	**85** *	1.24	**115** *	0.97	125	2.15
75	4.05	90	4.57	120	5.36	**130** *	1.76
80	10.99	95	10.38	125	9.75	135	5.67
Maintenance Dose							
WT = 50 kg (n = 1000)		WT = 60 kg (n = 1000)		WT = 80 kg (n = 1000)		WT = 90 kg (n = 1000)	
Dose (mg)	Err (%)	Dose (mg)	Err (%)	Dose (mg)	Err (%)	Dose (mg)	Err (%)
5	38.2	10	26.4	15	20.14	15	22.46
10	23.24	15	10.95	**20** *	7.13	20	11.49
15 *	3.94	**20** *	9.58	25	9.07	**25** *	2.29
20	22.37	25	33.92	30	27.66	30	18.41

3.5. Simulation

Given that only weight was the significant covariate, simulation for dose individualization was performed with the test dose allocated to 5 wt subgroups ranging between 50 and 90 kg. The resulting search processes were shown in Table 3. The deviations of simulated values from the target concentration, which was obtained as 29.9 mg/mL for $C_{Target,L}$ and 33.6 mg/mL for $C_{Target,M}$, were evaluated for each weight subgroup. The results suggested that to attain the target concentration, the loading dose must be increased by 15 mg for every 10 kg increment in body weight. Relatively less alterations would be needed for the maintenance dose, with 15 and 25 mg QD for the lowest and highest weight groups, respectively.

The above simulation results are visualized in Fig. 5 for the current standard dosing regimen (100 mg QD for 3 days for loading dose and 20 mg QD for maintenance dose) given for all weight groups (b) and the proposed optimal dosing regimen given for each weight group (c), along with the original data for the single dose of 40 mg given to all subjects revealing elevated concentrations in low body weight. The figure shows that large concentration deviations from the target concentration in low

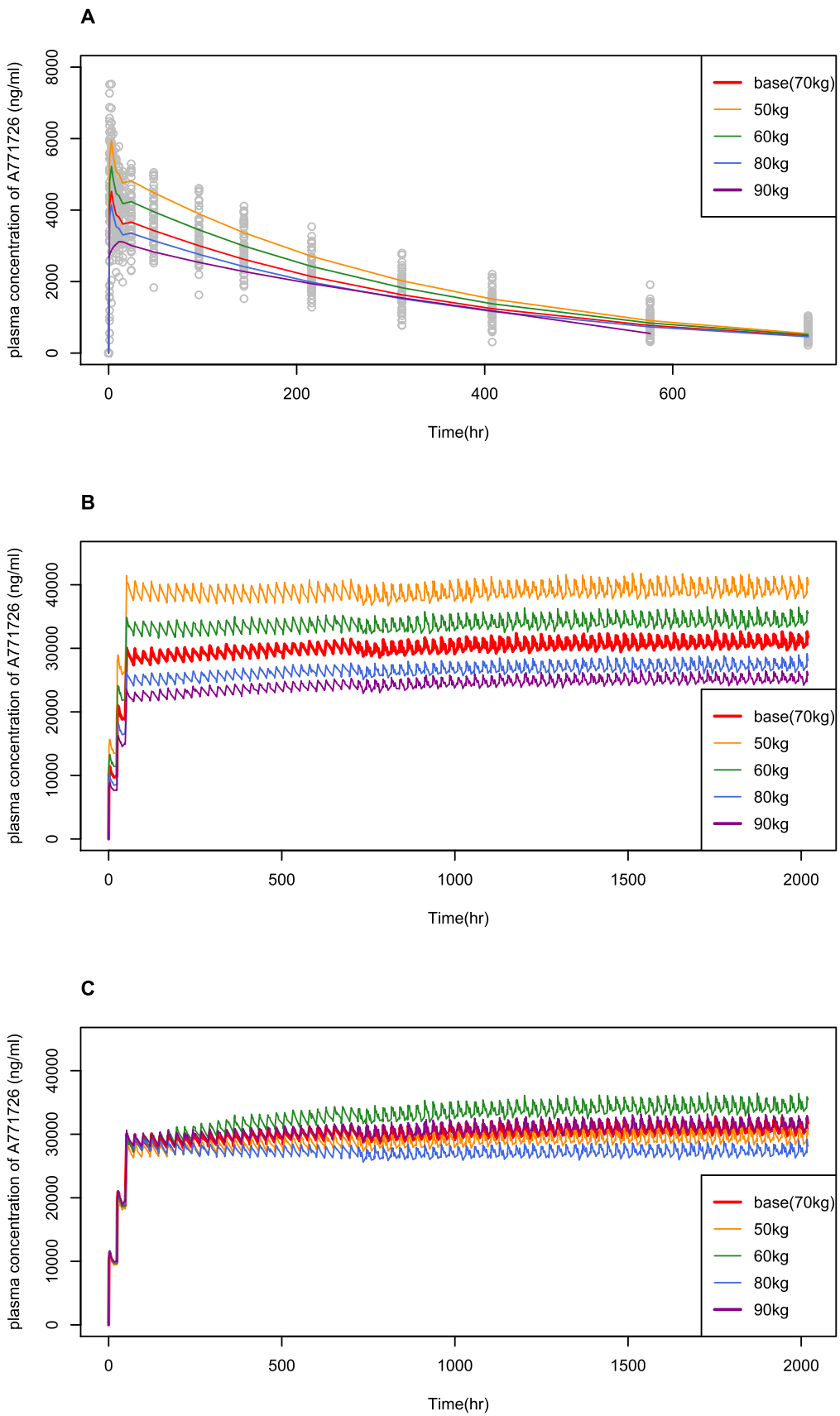

Fig. 5. A771726 concentration vs time profiles, stratified by weight (A) Observations (dots) and the mean observation (line) in each weight group for the original data, (B) Typical predictions in each weight group, given 100 mg QD loading dose followed by 20 mg QD maintenance dose, and (C) Typical predictions in each weight group, given optimal loading and maintenance doses.

and high weight groups disappear when the optimal doses are given, indicating the importance of dose individualization.

4. Discussion

In this study, we developed a population PK model for leflunomide in a Korean population. Based on the developed model, we proposed individualized dose regimens for different weight subgroups.

Our model successfully incorporated the mechanism related to EHC and showed significant improvements in model fit compared to the model without EHC included ($p = 0.007$) (data not shown).

As described in Methods and depicted in Fig. 2, leflunomide administrated into the gastric intestinal tract was assumed to subsequently enter the central compartment, which was then distributed into both peripheral and bile compartments. A771726 was assumed to accumulate in the gallbladder until its contraction and bile secretion upon food intake (Ibarra et al., 2021; Roberts et al., 2002). We assumed periodic intake of meals to accommodate the food-induced gallbladder emptying and estimated the duration of biliary secretion as a model parameter (T41) (Roberts et al., 2002).

During the model building process, we had to use some tricks to resolve numerical difficulties with fitting the model to the data. Because our data were obtained from PK studies, where blood samples were taken intensively in the early phase while taken sparsely in the late phase of the study, beginning Day 2, concentration data were available daily only, not hourly (see Data in the Methods section). This leads to almost no concentration data available at the meal times beginning Day 2. Hence, to solve for this problem, we used the following workaround.

- Step 1: Using the entire data, only ka, CL, Q, V2, and V3 were estimated.
- Step 2: Using the data only for the first 24 h (i.e., Day 1), with the above 4 parameter values fixed at their estimates obtained in Step 1, only k24 and T41 were estimated.
- Step 3: Using the entire data, with initial parameter estimates set at their estimates obtained in Step 1 and 2, all the parameters were estimated.

With this strategy, we were able to build the model successfully, although interindividual variability of some parameters was fixed at zero due to numerical issues.

A prior modeling work of leflunomide and teriflunomide based on the Chinese population (Yao et al., 2019) used a two-compartment disposition model, consisting of a central and a gallbladder compartment, in which EHC was described as a recycling process whereby the drug secreted from the gallbladder directly returned to the central compartment. In our study, however, we assumed that the drug was first secreted into the GI tract before reabsorbed. This model structure was better to accommodate the physiological mechanisms associated with EHC. The estimated PK parameter values of our model were overall larger than those estimated from the Chinese population. Compared to ka, CL, and V of 0.89 h^{-1}, 0.017 L/h, and 5.987 L in the Chinese population, respectively, our work showed that ka (= 1.61 h^{-1}) was 1.8 times as fast, CL (= 0.0273 L) 1.6 times as large, and V (= V2+V3 = 9.1 L) 1.5 times as large. This is likely due to the difference in the age distributions of the two different study populations.

Other than body weight implemented via allometric scaling, no significant covariate, including age, smoking, alcohol and caffeine, was identified, which is in concordance with previous findings (2012; Rozman, 2002; Sanofi-Aventis, 1998).

The data used in this work were obtained from clinical studies where a single dose of 40 mg leflunomide was given to subjects. Accordingly, the model so developed could not but be validated for a single dose of 40 mg only, as reported in Fig. 5. Taking this into account, we tried validating our model using data from previous studies where different doses were used. When validating the model using a single-dose case of 20 mg and a multiple-dose case of 50 mg loading doses for 3 days followed by 5 mg maintenance doses, we confirmed that in both cases concentration profiles simulated by our model were also similar to observed concentration profiles reported in previous studies (data not shown).

An important limitation of our study is the lack of pharmacogenetic information. The PK of leflunomide are reportedly affected by genetic polymorphism of ABCG2, CYP1A2 and CYP2C19×2 allele which may be associated with high inter-individual variability of ka in our model (Bohanec Grabar et al., 2009; Kim et al., 2011). In future studies, information related to such genomic polymorphism could be used to enhance the model predictability.

The previous dosing regimen suffered from increased treatment discontinuation due to side effects, with no progressive improvement in efficacy (Aletaha et al., 2003; Cutolo et al., 2013; Siva et al., 2003). For this reason, efforts were made to identify factors that might influence exposure-response and exposure-safety relationships of leflunomide metabolite, including age, sex, and liver function as well as pharmacogenetic differences. However, neither gender nor age affected dose adjustment (Shi et al., 2005; Rozman, 2002; Chan et al., 2005), which was also true in patients of juvenile rheumatoid arthritis. Thus, using the optimal dosing regimen proposed only by weight (Shi et al., 2005), the therapeutic range was set as 16 to 52 mg/L based on prior evidences (Fiehn et al., 2004; Metzler et al., 2004; van Roon et al., 2005; Williams et al., 2002). In our simulations, 50 and 90 kg weight groups included a significant number of subjects who showed deviations from this range when given the standard flat dose. When our weight-based optimal regimen was applied, the number of subjects that deviated from the therapeutic range decreased from 171 to 7 for a 50 kg weight group and from 33 to 15 for a 90 kg weight group.

In summary, the current recommended dosing regimen disregards the need for dose individualization and proposes a fixed dosing regimen of loading and maintenance doses of 100 mg QD and 20 mg QD, respectively, in all patients. Here, by applying a population PK based dose optimization approach with the target concentration set at the concentration expected in the 70 kg weight individual treated with the current recommended dosing regimen (i.e., 29.9 mg/L for loading dose and 33.6 mg/L for maintenance dose), we tried to demonstrate how the therapeutic concentration can be achieved in low and high WT individuals.

Since no significant differences of PK between healthy and RA patients are known (Rozman, 1998), it is expected that our optimal dosing scheme developed using healthy subjects could be similarly applied in RA patients for dose individualization.

5. Conclusions

This work demonstrates the importance of a population PK model-based dose optimization approach in maintaining drug therapeutic concentrations in leflunomide treatment.

CRediT authorship contribution statement

Yesong Shin: Formal analysis, Methodology, Software, Writing – original draft. **Dongwoo Chae:** Writing – review & editing. **Kyungsoo Park:** Conceptualization, Data curation, Investigation, Methodology, Project administration, Supervision, Writing – review & editing.

Declaration of Competing Interest

The authors declared no conflict of interest

Data availability

Data will be made available on request.

Acknowledgments

The authors acknowledge Seong Bok Jang at Yuhan Corporation for the curation of the data analyzed in this work while he was at Yonsei University.

This study was supported by a grant from the Brain Korea 21 Plus Project for Medical Science, Yonsei University. This research did not receive any specific grant from funding agencies in the public, commercial, or not-for-profit sectors.

The data used in this work cannot be open to the public because of hospital regulations. However, it is available upon a written request to the corresponding author.

Supplementary materials

Supplementary material associated with this article can be found, in the online version, at doi:10.1016/j.ejps.2023.106402.

Appendix

NONMEM code:

```
$PROB LEFLUNOMIDE PK
$INPUT ID TIME REALTIME DV WT AGE AMT CMT EVID MDV SMOKE ALC CAFF DVID
$DATA LEFLUNOMIDEFINISHED1REF_TIME_SD1.CSV;ACCEPT=(DVID.EQ.1)
$SUBROUTINE ADVAN13 TOL=13;NONLINEAR
$MODEL
NCOMPARTMENTS = 4
COMP = (DEPOT, DEFDOSE)
COMP = (CENTRAL, DEFOBS)
COMP = (PHERI)
COMP = (DUMMY); gal
$PK
TVCL = THETA(1)*(WT/70)**0.75
CL=TVCL*EXP(ETA(1)); Drug elimination clearance
TVV2 = THETA(2)*(WT/70)**1
V2=TVV2*EXP(ETA(2)); Volume of central compartment (C)
TVV3 = THETA(3)*(WT/70)**1
V3=TVV3*EXP(ETA(3)); Volume of peripheral compartment (P)
TVQ = THETA(4)*(WT/70)**0.75
Q=TVQ*EXP(ETA(4)); Distribution clearance
TVK12 = THETA(5)
K12=TVK12*EXP(ETA(5)); First order absorption/reabsorption rate constant
DUR=THETA(6)*EXP(ETA(6))
;K20 = CL/V2; First order elimination rate constant
K23 = Q/V2; First order central-to-peripheral rate constant
K32 = Q/V3; First order peripheral-to-central rate constant
K24 = THETA(7)*EXP(ETA(7)); First order secretion rate constant
FR = THETA(8)
;K42= THETA(9)
LLOQ=200
S2=V2
S3=V3
A_0(2)=0
A_0(3)=0
A_0(4)=0
$DES
MODT=MOD(TIME,24.0)
;DEFULT CONDITION
DADT(1) = -K12*A(1)
DADT(2) = K12*A(1) - (K23 + K24)*A(2) + K32*A(3) -(CL/V2)*A(2)*FR
DADT(3) = K23*A(2) - K32*A(3)-(CL/V3)*A(3)*(1-FR)
DADT(4) = K24*A(2)
IF (MODT>=4.AND.MODT<4+DUR) THEN
DADT(1) = -K12*A(1) + A(4)/DUR
DADT(2) = K12*A(1) - (K23 + K24)*A(2) + K32*A(3) -(CL/V2)*A(2)*FR
DADT(3) = K23*A(2) - K32*A(3)-(CL/V3)*A(3)*(1-FR)
DADT(4) = K24*A(2) - A(4)/DUR
ENDIF
IF (MODT>=10.AND.MODT<10+DUR) THEN
DADT(1) = -K12*A(1) + A(4)/DUR
DADT(2) = K12*A(1) - (K23 + K24)*A(2) + K32*A(3) -(CL/V2)*A(2)*FR
DADT(3) = K23*A(2) - K32*A(3)-(CL/V3)*A(3)*(1-FR)
DADT(4) = K24*A(2) - A(4)/DUR
ENDIF
IF (MODT>=23.AND.MODT<23+DUR) THEN
DADT(1) = -K12*A(1)+ A(4)/DUR
DADT(2) = K12*A(1) - (K23 + K24)*A(2) + K32*A(3) -(CL/V2)*A(2)*FR
DADT(3) = K23*A(2) - K32*A(3)-(CL/V3)*A(3)*(1-FR)
DADT(4) = K24*A(2) - A(4)/DUR
ENDIF
$ERROR
IPRED=F
Y=IPRED*(1+EPS(1))+EPS(2)
COMP_G = A(4) ;W = SQRT(THETA(9)**2*IPRED**2+THETA(10)**2)
Y = IPRED+ERR(1)*W
IRES = DV-IPRED
IWRES = IRES/W
$THETA
(0,0.0276,); CL
(0,6.85,); V2
(0,2.86,); V3
(0,0.75,); Q
(0,1.063,); K12
(0,7,); T41
(0,0.013,); K24
1 FIX; FR
(0, 0.02,); K42
$OMEGA
0.04;CL
0.09;V2
0 FIX;V3 plasma
0 FIX;Q
0.09;K12
0 FIX;DUR
0 FIX;K24
$SIGMA
0.01
10
$EST NSIG=3 PRINT=5 MAXEVAL=9999 METHOD=1 INTER NOABORT
$EST METHOD=IMP EONLY=1 PRINT=1 NITER=5 ISAMPLE=1000 MAPITER=0
$COV UNCONDITIONAL
$TABLE ID AMT TIME IPRED CWRES COMP_G CL V2 V3 Q K12 ETA1 ETA2 ETA3 ETA4 ETA5 ETA6 NOPRINT ONEHEADER FILE=ALLO_FULL_4
```

References

Leflunomide, LiverTox: Clinical and Research Information on Drug-Induced Liver Injury, 2012. Bethesda (MD).

Aletaha, D., Stamm, T., Kapral, T., Eberl, G., Grisar, J., Machold, K.P., Smolen, J.S., 2003. Survival and effectiveness of leflunomide compared with methotrexate and sulfasalazine in rheumatoid arthritis: a matched observational study. Ann. Rheum. Dis. 62, 944–951. https://doi.org/10.1136/ard.62.10.944.

Bohanec Grabar, P., Grabnar, I., Rozman, B., Logar, D., Tomsic, M., Suput, D., Trdan, T., Peterlin Masic, L., Mrhar, A., Dolzan, V., 2009. Investigation of the influence of CYP1A2 and CYP2C19 genetic polymorphism on 2-Cyano-3-hydroxy-N-[4-(*trifluoromethyl*)*phenyl*]-2-butenamide (A77 1726) pharmacokinetics in leflunomide-treated patients with rheumatoid arthritis. Drug Metab. Dispos. 37, 2061–2068. https://doi.org/10.1124/dmd.109.027482.

Chan, V., Charles, B.G., Tett, S.E., 2005. Population pharmacokinetics and association between A77 1726 plasma concentrations and disease activity measures following administration of leflunomide to people with rheumatoid arthritis. Br. J. Clin. Pharmacol. 60, 257–264. https://doi.org/10.1111/j.1365-2125.2005.02415.x.

Cutolo, M., Bolosiu, H., Perdriset, G., Group, L.S., 2013. Efficacy and safety of leflunomide in DMARD-naive patients with early rheumatoid arthritis: comparison of a loading and a fixed-dose regimen. Rheumatology (Oxford) 52, 1132–1140. https://doi.org/10.1093/rheumatology/kes321.

Fajardo-Robledo, N.S., Jacobo-Cuevas, H., Perez-Guerrero, E.E., Corona-Sanchez, E.G., Saldana-Cruz, A.M., Romero-Tejeda, E.M., Rodriguez-Jimenez, N.A., Totsuka-Sutto, S.E., Lopez-Roa, R.I., Ponce-Guarneros, J.M., Alcaraz-Lopez, M.F., Cerpa-Cruz, S., Munoz-Valle, J.F., Cardona-Munoz, E.G., Gonzalez-Lopez, L., Gamez-Nava, J.I., Therapeuti, R.G.F.R., 2022. Therapeutic response to leflunomide in combo therapy and monotherapy is associated to serum teriflunomide (A77 1726) levels. Sci. Rep. 12 https://doi.org/10.1038/s41598-022-05644-7.

Fiehn, C., Rochel, E., Ho, A.D., Max, R., 2004. Dose escalation of leflunomide (LEF) to 40 mg once daily in patients with rheumatoid arthritis and insufficient response to standard dose LEF. Ann. Rheum. Dis. 63, 746–747. https://doi.org/10.1136/ard.2003.014217.

Gastonguay, M.R., El-Tahtawy, A., Grp, M.R., 2005. Effect of nonmem minimization status and number of replicates on bootstrap parameter distributions for population pharmacokinetic models: a case study. Clin. Pharmacol. Ther. 77 https://doi.org/10.1016/j.clpt.2004.11.010. P2-P2.

Holford, N., Heo, Y.A., Anderson, B., 2013. A pharmacokinetic standard for babies and adults. J. Pharm. Sci. 102, 2941–2952. https://doi.org/10.1002/jps.23574.

Hopkins, A.M., Wiese, M.D., Proudman, S.M., O'Doherty, C.E., Foster, D., Upton, R.N., 2015. Semiphysiologically based pharmacokinetic model of leflunomide disposition in rheumatoid arthritis patients. CPT Pharmacometr. Syst. Pharmacol. 4, 362–371. https://doi.org/10.1002/psp4.46.

Ibarra, M., Trocóniz, I.F., Fagiolino, P., 2021. Enteric reabsorption processes and their impact on drug pharmacokinetics. Sci. Rep. 11, 5794. https://doi.org/10.1038/s41598-021-85174-w.

Kim, K.A., Joo, H.J., Park, J.Y., 2011. Effect of ABCG2 genotypes on the pharmacokinetics of A771726, an active metabolite of prodrug leflunomide, and association of A771726 exposure with serum uric acid level. Eur. J. Clin. Pharmacol. 67, 129–134. https://doi.org/10.1007/s00228-010-0916-0.

Metzler, C., Fink, C., Lamprecht, P., Gross, W.L., Reinhold-Keller, E., 2004. Maintenance of remission with leflunomide in Wegener's granulomatosis. Rheumatology 43, 315–320. https://doi.org/10.1093/rheumatology/keh009.

Mladenovic, V., Domljan, Z., Rozman, B., Jajic, I., Mihajlovic, D., Dordevic, J., Popovic, M., Dimitrijevic, M., Zivkovic, M., Campion, G., Musikic, P., Low-Friedrich, I., Oed, C., Seifert, H., Strand, V., 1995. Safety and effectiveness of leflunomide in the treatment of patients with active rheumatoid arthritis: results of a randomized, placebo-controlled, phase I1 study. Arthrit. Rheumat. 38, 1595–1603. https://doi.org/10.1002/art.1780381111.

Roberts, M.S., Magnusson, B.M., Burczynski, F.J., Weiss, M., 2002. Enterohepatic circulation: physiological, pharmacokinetic and clinical implications. Clin. Pharmacokinet. 41, 751–790. https://doi.org/10.2165/00003088-200241100-00005.

Rozman, B., 1998. Clinical experience with leflunomide in rheumatoid arthritis. Leflunomide Investigators' Group. J. Rheumatol. Suppl. 53, 27–32.

Rozman, B., 2002. Clinical pharmacokinetics of leflunomide. Clin. Pharmacokinet. 41, 421–430. https://doi.org/10.2165/00003088-200241060-00003.

Sanofi-Aventis, 1998. ARAVA(leflunomide) [FDA label] U.S. Food and Drug Administration website.

Shi, J., Kovacs, S.J., Wang, Y., Ludden, T.M., Bhargava, V.O., 2005. Population pharmacokinetics of the active metabolite of leflunomide in pediatric subjects with polyarticular course juvenile rheumatoid arthritis. J. Pharmacokinet. Pharmacodyn. 32, 419–439. https://doi.org/10.1007/s10928-005-0049-8.

Siva, C., Eisen, S.A., Shepherd, R., Cunningham, F., Fang, M.A., Finch, W., Salisbury, D., Singh, J.A., Stern, R., Zarabadi, S.A., 2003. Leflunomide use during the first 33 months after food and drug administration approval: experience with a national cohort of 3,325 patients. Arthrit. Rheum.-Arthr. 49, 745–751. https://doi.org/10.1002/art.11452.

Soulele, K., Karalis, V., 2019. On the population pharmacokinetics and the enterohepatic recirculation of total ezetimibe. Xenobiotica 49, 446–456. https://doi.org/10.1080/00498254.2018.1463117.

van Roon, E.N., Jansen, T.L., van de Laar, M.A., Janssen, M., Yska, J.P., Keuper, R., Houtman, P.M., Brouwers, J.R., 2005. Therapeutic drug monitoring of A77 1726, the active metabolite of leflunomide: serum concentrations predict response to treatment in patients with rheumatoid arthritis. Ann. Rheum. Dis. 64, 569–574. https://doi.org/10.1136/ard.2004.025205.

W. Weber, L.H., 1997. Use of a Population Approach to the Development of Leflunomide: A New Disease-Modifying Drug in the Treatment of Rheumatoid Arthritis. Hoechst Marion Roussel. COST B1 medicine, Geneva, pp. 239–244.

Weinblatt, M.E., Kremer, J.M., Coblyn, J.S., Maier, A.L., Helfgott, S.M., Morrell, M., Byrne, V.M., Kaymakcian, M.V., Strand, V., 1999. Pharmacokinetics, safety, and efficacy of combination treatment with methotrexate and leflunomide in patients with active rheumatoid arthritis. Arthrit. Rheum. 42, 1322–1328. https://doi.org/10.1002/1529-0131(199907)42:7<1322::AID-ANR4>3.0.CO;2-P.

West, G.B., Brown, J.H., Enquist, B.J., 1997. A general model for the origin of allometric scaling laws in biology. Science 276, 122–126. https://doi.org/10.1126/science.276.5309.122.

Williams, J.W., Mital, D., Chong, A., Kottayil, A., Millis, M., Longstreth, J., Huang, W., Brady, L., Jensik, S., 2002. Experiences with leflunomide in solid organ transplantation. Transplantation 73, 358–366. https://doi.org/10.1097/00007890-200202150-00008.

Yao, X., Wu, Y., Jiang, J., Chen, X., Liu, D., Hu, P., 2019. A population pharmacokinetic study to accelerate early phase clinical development for a novel drug, teriflunomide sodium, to treat systemic lupus erythematosus. Eur. J. Pharm. Sci. 136, 104942 https://doi.org/10.1016/j.ejps.2019.05.020.